ANNALS of Clinical and Translational Neurology
Open Access
AMERICAN NEUROLOGICAL ASSOCIATION

RESEARCH ARTICLE

MRI evidence of gray matter loss in COVID-19 patients with cognitive and olfactory disorders

Serena Capelli[1], Alberto Arrigoni[1], Angela Napolitano[2], Giulio Pezzetti[2], Andrea Remuzzi[3], Rosalia Zangari[4], Ferdinando Luca Lorini[5], Maria Sessa[6], Anna Caroli[1] & Simonetta Gerevini[2]

[1]Bioengineering Department, Istituto di Ricerche Farmacologiche Mario Negri IRCCS, Ranica, BG, Italy
[2]Department of Neuroradiology, ASST Papa Giovanni XXIII, Bergamo, Italy
[3]Department of Management, Information and Production Engineering, University of Bergamo, Dalmine, BG, Italy
[4]FROM Research Foundation, ASST Papa Giovanni XXIII, Bergamo, Italy
[5]Department of Emergency and Critical Care Area, ASST Papa Giovanni XXIII, Bergamo, Italy
[6]Department of Neurology, ASST Papa Giovanni XXIII, Bergamo, Italy

Correspondence
Anna Caroli, Bioengineering Department, Istituto di Ricerche Farmacologiche Mario Negri IRCCS, Via G. B. Camozzi, 3, Ranica 24020, BG, Italy. Tel: +39 035 4535381; Fax: +39 035 4535371; E-mail: anna.caroli@marionegri.it.

Received: 21 June 2024; Revised: 10 July 2024; Accepted: 12 July 2024

***Annals of Clinical and Translational Neurology* 2024; 11(9): 2457–2472**

doi: 10.1002/acn3.52164

Abstract

Objective: The aim of this study was to assess COVID-19-related gray matter (GM) structural alterations in two distinct groups of patients presenting with the prevailing and distinctive COVID-19-related neurological symptoms – isolated olfactory disorders as sole neurological manifestation (COVID-OD) and cognitive disorders (COVID-CD) – as compared to a control group of unaffected individuals. **Methods**: The study included 61 COVID-CD patients (57 [60–63] years, 62% females), 84 COVID-OD patients (49 [35–57] years, 60% females), and 17 controls (51 [41–52] years, 41% females). Region-based morphometry (RBM) and voxel-based morphometry (VBM) were performed on T1-weighted MRI scans to assess GM regional volume and voxel-wise density differences between COVID-19 patients and controls. Surface-based morphometry (SBM) was applied to investigate cortical thickness alterations. The statistical models built to assess GM structural differences among groups included total intracranial volume and age as nuisance variables. **Results**: The multi-morphometric analysis revealed statistically significant ($p < 0.05$ corrected for multiple comparisons) reduction in GM regional volumes, in voxel-wise GM density and in cortical thickness in both COVID-CD and COVID-OD patient groups as compared to controls. Across all three analyses, COVID-CD patients showed more distributed and severe GM loss than COVID-OD patients. The most prominently affected GM regions in the COVID-CD group included the hippocampus, putamen, cingulate gyrus, precuneus, precentral and postcentral gyri, amygdala, lingual gyrus, and caudate nucleus. **Interpretation**: Our MRI findings show that COVID-19-related olfactory and cognitive disorders both induce GM atrophy, although at different degrees of severity, likely indicative of neurodegeneration and neuroinflammation.

Introduction

In the 3 years since the initial outbreak of coronavirus disease 2019 (COVID-19), caused by the severe acute respiratory syndrome coronavirus 2 (SARS-CoV-2), increasing scientific evidence has emerged, shedding light on the extensive impact of this viral infection beyond its primary respiratory manifestations. Notably, a growing body of research has provided evidence that SARS-CoV-2 affects the central nervous system (CNS), giving rise to a spectrum of neurological consequences.[1–14]

A wide range of neuroimaging alterations have been reported in COVID-19 patients,[15–21] and the relevance of brain magnetic resonance imaging (MRI) in assessing

© 2024 The Author(s). *Annals of Clinical and Translational Neurology* published by Wiley Periodicals LLC on behalf of American Neurological Association. This is an open access article under the terms of the Creative Commons Attribution-NonCommercial-NoDerivs License, which permits use and distribution in any medium, provided the original work is properly cited, the use is non-commercial and no modifications or adaptations are made.

both structural and functional cerebral changes occurring in COVID-19 patients with neurological symptoms has become increasingly evident.[22–29]

One of the most prevalent – reported in about 40%[30] of cases – and distinctive neurological symptoms associated with COVID-19 is olfactory loss, typically occurring as hyposmia (or hypogeusia), anosmia (or ageusia), or dysosmia (or dysgeusia). This symptom frequently occurs early in the disease, also in patients who are otherwise oligosymptomatic or even asymptomatic, and it can persist after other symptoms have subsided.

Although widely reported, the specific pathophysiological mechanism underlying olfactory loss in COVID-19 is still unclear. Previous studies showed that this symptom is not linked to nasal obstruction or rhinitis. Instead, it may be attributed to the virus's neurotropism: angiotensin-converting enzyme 2 (ACE2) is widely present in the olfactory system and, serving as a viral receptor, it may provide SARS-CoV-2 access to the CNS.[31,32] Propagation of viruses by retrograde axonal transport to the olfactory bulbs and to the CNS has also been described.[33] Such interpretation is also supported by one of our earlier studies in which significant olfactory bulbs' atrophy was found in COVID-19 patients experiencing neurological complications, as compared with normal controls.[26]

Among the neurological manifestations of COVID-19, cognitive impairment, occurring in the acute phase and/or persisting after resolution of the disease, is one of the most concerning. Cognitive disorders include difficulty concentrating, confusion, forgetfulness, tip-of-the tongue word-finding problems, semantic disfluency, diminished alertness or mental sharpness, and attention deficits.[34–36] They are often referred to as "brain fog," a nonmedical term widely used to indicate such a state of "clouded consciousness."[37]

Also in this case, the precise mechanisms underlying cognitive disorders in COVID-19 are not fully understood. Previous studies[25] reported alterations in brain diffusivity in COVID-19 patients with neurological disorders (including cognitive decline), especially in the white matter (WM), suggesting a massive microglia activation following SARS-Cov-2 infection, prompting neuroinflammation and ultimately causing cerebral damage.

The link between cognition and gray matter (GM) structures is well-established in neuroscience, as many cross-sectional and longitudinal studies have demonstrated clear relationships between cognitive decline and the atrophy of specific brain regions, both in normal aging and in neurodegenerative diseases.[38–43] Over the past decade, GM volume and cortical thickness have emerged as relevant biomarkers for brain development, aging, and plasticity, and to monitor the evolution of a number of neurological diseases.[44–47]

Brain volume is commonly assessed in vivo, noninvasively, using high-resolution T1-weighted MRI scans. GM regional atrophy can be quantified by region-based morphometry (RBM), a technique providing the volume of individual regions of interest (ROI), based on their a priori definition by manual segmentation or atlas parcellation.[48,49] Voxel-based morphometry (VBM) allows to investigate whole-brain differences in GM density, voxel-wise, without focusing on a priori-defined ROIs.[48,50–53] In addition, surface-based morphometry (SBM) is specifically designed for evaluating cortex morphology[54] and in particular allows to assess cortical thickness (also referred to as cortical depth) by measuring the voxel- or surface-based distance between the inner and outer boundaries of the GM ribbon.[44]

Previous studies investigating brain morphometry in COVID-19 revealed GM loss in patients developing a wide range of neurological symptoms,[55–60] and a few studies reported cortical thinning.[61,62]

The objective of this study was to explore COVID-19-related GM structural alterations using a multi-morphometric approach encompassing GM volume and cortical thickness analysis. Two distinct groups of patients were investigated, representing the prevailing and distinctive COVID-19-related neurological symptoms: (i) isolated olfactory disorders as sole neurological manifestation, and (ii) cognitive disorders – and compared to a control group of unaffected individuals. To the best of our knowledge, a comprehensive investigation of GM structural alterations in these well-characterized COVID-19 patient subgroups has not been previously performed, and could complement previous evidence, providing additional insight into the multifaceted impact of COVID-19 on the brain.

Methods

Patient population

This is a retrospective, observational study. Individuals with confirmed COVID-19 and related neurological disorders who underwent brain MRI at ASST Papa Giovanni XXIII hospital in Bergamo, Italy, between March 2020 and October 2021, were considered eligible for participation.

The confirmation of COVID-19 diagnosis followed one of the following criteria: (1) nasopharyngeal specimens testing positive for the virus using real-time reverse-transcriptase polymerase chain reaction (RT-PCR); or (2) bronchoalveolar lavage (BAL) samples being positive for SARS-CoV-2 by RT-PCR in cases where there was a strong clinical suspicion of infection, along with negative results from at least two nasopharyngeal swabs

 © 2024 The Author(s). *Annals of Clinical and Translational Neurology* published by Wiley Periodicals LLC on behalf of American Neurological Association.

taken at least 24 hours apart; or (3) presence of radiological signs of interstitial pneumonia consistent with characteristic symptoms (such as fever, dry cough, and difficulty breathing), even with negative RT-PCR test.

Subjects with preexisting neurological disorders (e.g., multiple sclerosis, previous vascular lesions, and psychiatric conditions) and/or preexisting brain tissue abnormalities (e.g., chronic stroke and tumors) were excluded. Additionally, individuals who exhibited cerebrovascular disorders with brain tissue abnormalities (e.g., stroke, cerebral venous thrombosis) following COVID-19 were also excluded.

From the pool of patients who fulfilled the inclusion criteria, individuals who exhibited isolated olfactory disorders (OD) as their sole neurological manifestation were grouped and referred to as COVID-OD. Among the remaining patients who presented with other neurological disorders (with or without olfactory disorders), those with cognitive disorders (CD) as the primary neurological manifestation were grouped and referred to as COVID-CD.

OD was intended as a self-reported reduced or distorted ability to smell during sniffing (orthonasal olfaction) and/or eating (retronasal olfaction),[63] while CD included confusion, memory impairment, delirium, hallucinations, and attention deficits.

The flowchart (Fig. 1) provides a visual representation of the steps involved in patient recruitment and subgroup assignment.

Individuals with no prior record of COVID-19 (including confirmed diagnosis or symptoms related to COVID-19) and no reported impairment in their sense of smell or taste, who underwent brain MRI at the Neuroradiology Department of the Bergamo hospital for reasons unrelated to COVID-19 complications and exhibited unremarkable MRI findings were included in the study as normal controls.

The use of patient data was granted ethical approval by the local ethics committee as part of a broader observational study protocol (Reg. 118/22). Informed consent was acquired from patients or from their next of kin (in the case of ICU patients).

MRI acquisition

Both COVID-19 patients and controls underwent brain MRI at the Neuroradiology Department of the ASST Papa Giovanni XXIII hospital in Bergamo, Italy, on a 3-Tesla MRI scanner manufactured by General Electric (Discovery MR 750w GEM).

A T1-weighted scan was acquired using an axial Multi Echo Multi Planar (MEMP) sequence, using the following parameters: matrix = 288 × 244, field of view = 250 × 250 mm, thickness/gap = 3.0/0.4 mm, TE/TR = 9/600 ms (COVID-19 patients) and matrix = 320 × 256, field of view = 250 × 250 mm, thickness/gap = 4.0/0.4 mm, TE/TR = 480/9 ms (control subjects).

MRI processing

To perform RBM, VBM, and SBM, the CAT12 toolbox (Computational Anatomy Toolbox 12, http://www.neuro.uni-jena.de/cat/) was used. CAT12 is a computational framework developed by the Structural Brain Mapping Group at the Departments of Psychiatry and Neurology of the Jena University Hospital, Germany, running as a toolbox in SPM12 (Statistical Parametric Mapping, Wellcome Centre for Human Neuroimaging, UCL Queen Square Institute of Neurology, London, UK), and its routines are implemented in MATLAB (Natick, MA, USA). CAT12, SPM12, and MATLAB versions used for this study were 2170 CAT12.8.2, v7771, and R2022b, respectively.

RBM and VBM were performed to assess GM regional volume and voxel-wise density differences, respectively, between COVID-19 patients and controls, while SBM was applied to investigate the cortical thickness.

The technical details of preprocessing procedures performed with CAT12 are described in prior publications.[54] Briefly, they include application of a spatial adaptive non-local means (SANLM) denoising filter, bias correction, and affine registration, followed by brain skull-stripping, and the final adaptive maximum a posteriori (AMAP) segmentation.[64] Segmentations are finally refined by applying a partial volume estimation[65] and the tissue segments are spatially normalized to the standard MNI space using Geodesic Shooting registrations.[66]

When performing SBM with CAT12, preprocessing includes the cortical thickness estimation and reconstruction of the central surface, which occurs in one step using a projection-based thickness (PBT) method.[67] Topological correction and surface refinement are also performed. As a last step, the local thickness values are transferred onto the Freesurfer "FsAverage" template (Athinoula A. Martinos Center for Biomedical Imaging, Charlestown, Massachusetts, USA).

After preprocessing, prior to conducting the statistical analyses, GM segmentations were spatially smoothed using a Gaussian kernel to reduce individual variance and ensure normal distribution of the data, thereby increasing the validity of parametric statistical tests. For GM volume analysis (RBM and VBM), full width at half maximum (FWHM) of the Gaussian kernel was set to 8 mm. Similarly, the cortical thickness maps (SBM) were smoothed with a 12 mm Gaussian kernel.

During preprocessing, total intracranial volume (TIV), that is the overall volume, in cubic millimeters, of the

© 2024 The Author(s). *Annals of Clinical and Translational Neurology* published by Wiley Periodicals LLC on behalf of American Neurological Association.

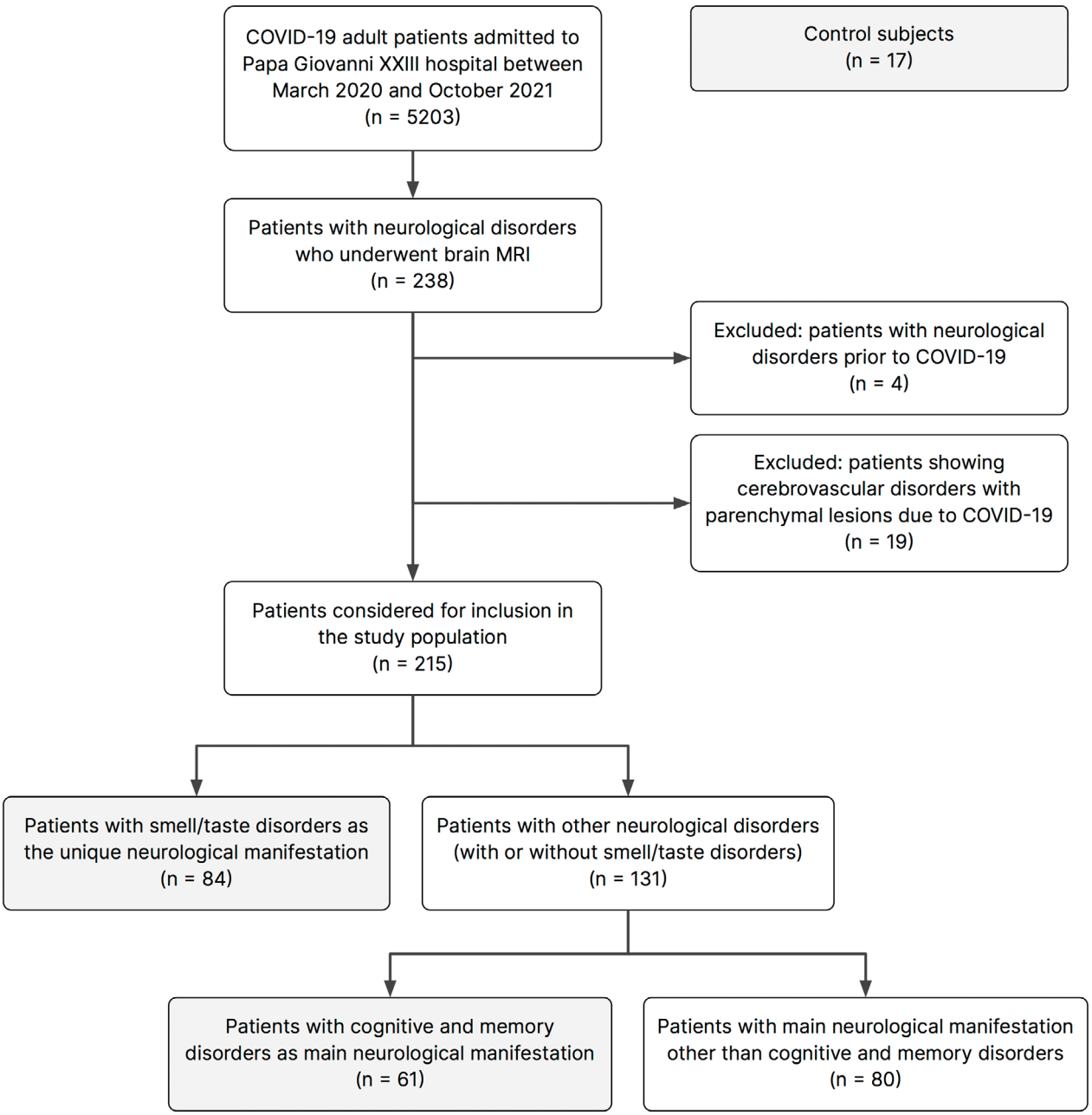

Figure 1. Flowchart providing visual representation of patients and controls recruitment, exclusion criteria, and subgroup assignment. Gray-filled boxes indicate the patient and control groups ultimately included in the study.

space within the skull, was calculated for each subject. GM, WM, and CSF volumes were also computed.

The Neuromorphometrics atlas (Neuromorphometrics, Inc. http://Neuromorphometrics.com/) was used in this study for the evaluation of GM volume and density (in both RBM and VBM) due to its high level of detail with 138 cortical and subcortical structures, its integration with the CAT12 toolbox, and its wide validation and use in the neuroimaging community. The Desikan-Killiany atlas[68] was utilized in the assessment of cortical thickness with SBM.

Statistical analysis

Wilcoxon rank-sum test was employed to assess differences in age, TIV, and GM volume between the control

 © 2024 The Author(s). *Annals of Clinical and Translational Neurology* published by Wiley Periodicals LLC on behalf of American Neurological Association.

group and each COVID-19 patient subgroup. Pairwise comparisons in terms of sex were performed with the Fisher test. R software (R Core Team, Vienna, Austria, https://www.r-project.org/) version 4.2.2 was used for such statistical analyses.

To compare GM volume and cortical thickness between controls and each COVID-19 subgroup, the general linear model (GLM) approach implemented in CAT12 was employed.[69] Among the statistical tests available in CAT12, the two-sample t-test was chosen to assess statistical significance.

While assessing GM volume (in both RBM and VBM analyses), TIV and age were included as nuisance variables in order to remove the related variance. Sex was not included as covariate in the GLM, as it has been shown that adjusting data using TIV eliminate differences due to sex.[70,71]

Given that cortical thickness does not exhibit scaling proportional to brain size, as established by Barnes et al.,[72] correction for TIV was not employed in the SBM analysis, and age was included as the only nuisance variable in the GLM.

To account for multiple comparisons, the false discovery rate (FDR) method was utilized to adjust the results of RBM (level of significance: p_{FDR} <0.05), as brain regions are correlated and the family-wise error method (FWE) could have been too conservative.[73] VBM and SBM results were corrected for multiple comparisons with the family-wise error method (FWE) applying a significance level of p_{FWE} <0.05 at the peak level.

In both VBM and SBM, cluster-extent based thresholding was applied to exclude results stemming from noise and control for false-positives. The threshold was empirically defined relying on the expected number of voxels per cluster automatically computed during model estimation.

Results

A total of 84 COVID-19 patients with olfactory loss as the only neurological disorder (COVID-OD), 61 COVID-19 patients with cognitive disorders as the main neurological manifestation (COVID-CD), and 17 control participants were enrolled in the study. Within the COVID-CD cohort, 19 patients also reported various forms of olfactory disorders such as anosmia, hyposmia, dysosmia, ageusia, hypogeusia, or cacosmia.

Demographic features, TIV, and normalized GM volume in the COVID-CD, COVID-OD, and control patients included in the study are summarized in Table 1.

COVID-CD patients were significantly older than controls (57 [50–63] vs. 51 [41–52] years, respectively; $p = 0.003$) and than COVID-OD patients (57 [50–63] years vs. 49 [35–57] years, $p < 0.001$). Age did not differ between COVID-OD patients and controls ($p = 0.989$).

Table 1. Demographic features, total intracranial volume, and gray matter volume in the COVID-CD patients, COVID-OD patients, and control subjects included in the study.

	COVID-CD	COVID-OD	Control
n	61	84	17
Age, years	57 [50–63]*	49 [35–57]	51 [41–52]
Sex, F	38 (62%)	50 (60%)	7 (41%)
TIV, mL[#]	1398 [1303–1483]	1431 [1344–1536]	1513 [1385–1568]
Normalized GM volume[##]	0.383 [0.361–0.404]	0.401 [0.383–0.427]	0.393 [0.390–0.414]

Data are shown as median [IQR] or number (%). Pairwise comparisons between each patient group and controls were performed by Wilcoxon rank-sum test – independent samples test (continuous variables) or Fisher's test (binary variables). *$p < 0.05$. [#]corrected for sex; [##]corrected for age and sex, normalized by TIV.
Abbreviations: GM, gray matter; OD, olfactory dysfunction; CD, cognitive disorders; TIV, total intracranial volume.

There were no statistically significant differences in terms of sex, TIV (corrected for sex), and normalized GM volume (computed as wholebrain GM volume/TIV ratio and corrected for age and sex), between each patient group and the control group.

The MRI time, defined as number of days between COVID-19 onset and MRI acquisition, was not statistically significantly different between the COVID-CD and COVID-OD patient groups (210 [53–446] vs. 237 [180–323] days, $p = 0.346$).

Regional gray matter atrophy: RBM Results

Out of the 138 GM regions encompassing the cortex and the main subcortical structures within the Neuromorphometrics atlas (Neuromorphometrics, Inc. http://Neuromorphometrics.com/), a total of 73 regions exhibited significant atrophy in COVID-CD patients compared to controls ($p < 0.05$, FDR-corrected, age and TIV adjusted volumes). In the COVID-OD group, only 41 GM regions showed significant atrophy compared to the control group ($p < 0.05$, FDR-corrected, with adjustments for age and TIV).

Figure 2 illustrates the color-coded representation of GM regions based on the statistical significance of volume reduction. Table 2 provides a summary of the most significant regions ($p < 0.001$, FDR-corrected, age and TIV adjusted volumes) while a comprehensive list of regions displaying significant atrophy ($p < 0.05$, FDR-corrected, with age and TIV adjustment), can be found in Tables S1 and S2.

© 2024 The Author(s). *Annals of Clinical and Translational Neurology* published by Wiley Periodicals LLC on behalf of American Neurological Association.

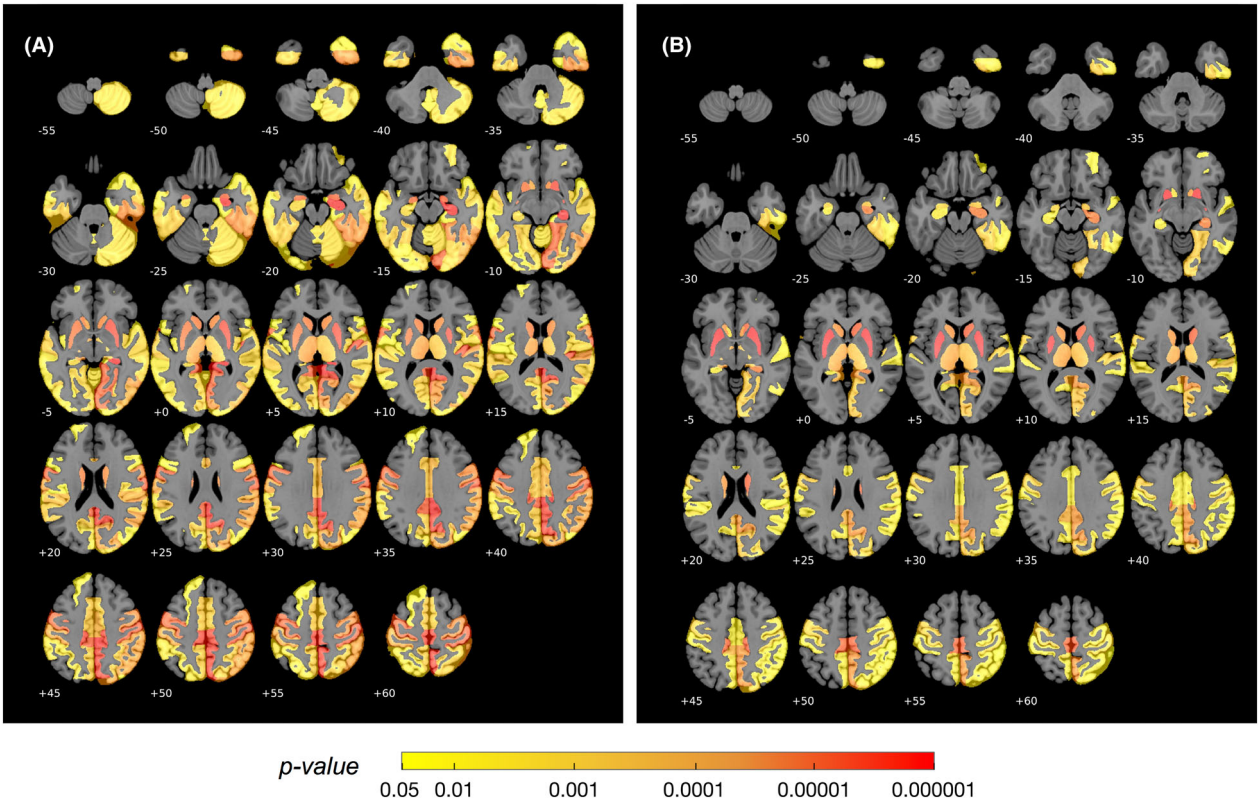

Figure 2. Gray matter regions with statistically significant atrophy in the 61 COVID-19 patients with cognitive disorders (COVID-CD) (A) and the 84 COVID-19 patients with olfactory dysfunction (COVID-OD) (B), as compared to controls. Gray matter regions were defined using the Neuromorphometrics atlas (Neuromorphometrics, Inc. http://Neuromorphometrics.com/) and color-coded based on the statistical significance (FDR-corrected *p*-value <0.05) of the atrophy. The color-coded findings are overlaid on the axial sections of the MNI152 brain template.

All 41 GM regions showing statistically significant atrophy in the COVID-OD group also exhibited a significant atrophy in the COVID-CD group. However, in 25 out of these 41 regions, GM atrophy in the COVID-CD group was significantly more severe than in the COVID-OD group (Table S3, Fig. S1).

Conversely, no regions showed a statistically significant increase in GM volume in either the COVID-CD or the COVID-OD group, as compared to controls.

Gray matter density: VBM Results

In the whole-brain VBM analysis, 12 clusters (extent threshold = 100 voxels) of statistically significant GM loss were observed in COVID-CD patients as compared to controls ($p < 0.05$, FWE-corrected). The statistical peaks of the largest clusters are located in the right fusiform gyrus, the right putamen, and the medial segment of the precentral gyrus.

In the COVID-OD group, the VBM analysis unveiled statistically significant GM reduction in 12 clusters (extent threshold = 100 voxels) as compared to controls ($p < 0.05$, FWE-corrected). The statistical peaks of the largest clusters are located bilaterally in the putamen and in the left thalamus.

Differences between patient groups and controls are reported in terms of T-statistics in Table 3 and graphically represented through statistical maps reporting the T-values in Figure S2, centered on the three largest clusters.

No statistically significant increase in GM density was found in either the COVD-CD or the COVID-OD group, as compared to controls.

Cortical thickness: SBM results

The vertex-wise cortical thickness analysis showed significant cortical thinning in COVID-CD patients as compared to controls, in both brain hemispheres, especially in the medial parts. Twenty-five clusters of vertices were found to have significantly thinner cortex ($p < 0.05$, FWE-corrected, cluster-extent threshold = 20 vertices).

 © 2024 The Author(s). *Annals of Clinical and Translational Neurology* published by Wiley Periodicals LLC on behalf of American Neurological Association.

Table 2. Differences in regional gray matter volume between COVID-19 patient groups and the control population.

ROI	COVID-CD	Control	*p*
R hippocampus	2.509 [2.172–2.769]	3.138 [2.961–3.348]	<0.0001
R posterior cingulate gyrus	2.317 [2.141–2.521]	3.042 [2.880–3.111]	<0.0001
R putamen	1.575 [1.389–1.821]	2.197 [1.795–2.602]	<0.0001
R precentral gyrus (medial segment)	1.410 [1.257–1.684]	1.958 [1.726–2.135]	<0.0001
L precentral gyrus (medial segment)	1.490 [1.256–1.709]	2.034 [1.899–2.164]	<0.0001
R precuneus	6.882 [6.236–7.570]	8.553 [8.066–8.733]	<0.0001
R transverse temporal gyrus	0.779 [0.707–0.869]	1.068 [0.985–1.136]	<0.0001
R postcentral gyrus	5.803 [5.278–6.514]	7.261 [6.781–7.486]	<0.0001
L posterior cingulate gyrus	2.618 [2.366–2.899]	3.507 [3.027–3.627]	<0.0001
R amygdala	0.588 [0.538–0.662]	0.782 [0.738–0.831]	<0.0001
R lingual gyrus	4.719 [4.387–5.109]	5.601 [5.097–6.474]	<0.0001
L precentral gyrus	7.333 [6.687–8.350]	9.341 [8.693–10.36]	<0.0001
L amygdala	0.639 [0.559–0.694]	0.791 [0.734–0.888]	<0.0001
L putamen	1.723 [1.463–1.925]	2.008 [1.664–2.631]	<0.0001
L caudate	1.353 [0.937–1.573]	2.071 [1.683–2.271]	< 0.0001
R accumbens area	0.232 [0.181–0.256]	0.297 [0.255–0.347]	<0.0001
R caudate	1.497 [1.089–1.773]	2.280 [1.920–2.690]	<0.0001
R precentral gyrus	6.918 [6.114–8.039]	8.793 [8.198–9.807]	<0.0001
R fusiform gyrus	5.185 [4.550–4.488]	6.159 [5.907–6.507]	0.0001
R calcarine cortex	1.349 [1.089–1.641]	1.911 [1.626–2.313]	0.0002
R inferior temporal gyrus	8.123 [7.348–8.713]	9.845 [8.530–10.120]	0.0002
R planum temporale	1.263 [1.196–1.419]	1.587 [1.413–1.724]	0.0002
L thalamus proper	2.566 [2.136–3.08]	3.592 [2.861–3.951]	0.0002
R supramarginal gyrus	5.182 [4.697–5.649]	6.315 [6.016–6.667]	0.0003
R cuneus	2.564 [2.317–2.817]	3.36 [2.903–3.466]	0.0003
R angular gyrus	7.184 [6.546–7.780]	8.503 [7.605–9.141]	0.0003
R superior occipital gyrus	2.606 [2.252–2.757]	2.963 [2.842–3.212]	0.0003
L postcentral gyrus	6.622 [6.212–7.457]	8.191 [7.276–8.853]	0.0004
L accumbens area	0.242 [0.205–0.266]	0.310 [0.252–0.363]	0.0004
R inferior occipital gyrus	3.914 [3.497–4.327]	4.657 [4.335–5.248]	0.0006

ROI	COVID-OD	Control	*p*
R putamen	1.609 [1.435–1.822]	2.197 [1.795–2.602]	<0.0001
L putamen	1.721 [1.504–1.899]	2.008 [1.664–2.631]	<0.0001
R caudate	1.753 [1.406–2.010]	2.280 [1.920–2.690]	<0.0001
R precentral gyrus (medial segment)	1.532 [1.374–1.698]	1.958 [1.726–2.135]	<0.0001
L precentral gyrus (medial segment)	1.574 [1.410–1.787]	2.034 [1.899–2.164]	<0.0001
R hippocampus	2.689 [2.368–2.924]	3.138 [2.961–3.348]	< 0.0001
L caudate	1.647 [1.271–1.868]	2.071 [1.683–2.271]	0.0002
R precuneus	7.535 [6.791–8.025]	8.553 [8.066–8.733]	0.0002
R posterior cingulate gyrus	2.468 [2.306–2.696]	3.042 [2.88–3.111]	0.0002
R accumbens area	0.254 [0.216–0.283]	0.297 [0.255–0.347]	0.0003
L thalamus proper	2.745 [2.174–3.251]	3.592 [2.861–3.951]	0.0003

GM ROIs were defined using the Neuromorphometrics atlas (Neuromorphometrics, Inc. http://Neuromorphometrics.com/). Volumes are in mL and shown as median [IQR]. TIV and age were included as covariates in the GLM. Only brain regions displaying the most pronounced and statistically significant reduction in volume ($p < 0.001$, FDR-corrected) in COVID groups as compared to controls are shown. The comprehensive list of 73 GM regions exhibiting a significant decrease in volume ($p < 0.05$, FDR-corrected) identified through the RBM analysis are reported in Table S1.
Abbreviations: CD, cognitive disorders; FDR, false discovery rate; GLM, general linear model; GM, gray matter; L, left; OD, olfactory disorders; R, right; RBM, region-based morphometry; TIV, total intracranial volume.

The statistical peaks of the largest clusters with significantly thinner cortex are located bilaterally in the paracentral lobule and within the right lingual gyrus.

The SBM analysis unveiled significant cortical thinning also in the COVID-OD group as compared to controls. Eleven clusters were found to have significantly lower

© 2024 The Author(s). *Annals of Clinical and Translational Neurology* published by Wiley Periodicals LLC on behalf of American Neurological Association.

Table 3. Clusters of gray matter voxels with significant volume reduction in the patient groups as compared to controls (cluster $p < 0.05$, FWE-corrected; extent threshold = 100 voxels).

	Peak MNI coordinates (mm)					
Cluster size	*x*	*y*	*z*	Region	*T*	*p*
COVID-CD						
16627	23	−48	−13	R fusiform gyrus	8.48	<0.001
	4	−21	50	R precentral gyrus (medial segment)	7.97	< 0.001
	−2	−28	46	L posterior cingulate gyrus	7.06	<0.001
1958	25	6	−5	R putamen	6.59	<0.001
1888	−2	−26	52	L precentral gyrus (medial segment)	8.14	<0.001
	−3	−19	48	L precentral gyrus (medial segment)	6.45	<0.001
	−3	−20	64	L precentral gyrus (medial segment)	6.45	<0.001
901	52	−17	52	R postcentral gyrus	6.36	<0.001
	58	−11	43	R postcentral gyrus	5.45	0.009
830	41	−25	12	R postcentral gyrus	7.25	<0.001
726	−22	7	−7	L putamen	5.87	0.002
593	−23	−25	64	L precentral gyrus	6.03	0.001
	−20	−22	75	L precentral gyrus	5.47	0.008
410	25	−24	64	R precentral gyrus	5.88	0.001
	24	−24	73	R precentral gyrus	5.54	0.007
397	−9	2	10	L caudate	6.00	0.001
	−6	16	1	L caudate	5.66	0.004
	−11	−7	17	L thalamus	5.60	0.005
376	6	−14	30	R middle cingulate gyrus	6.86	<0.001
	−4	−15	29	L middle cingulate gyrus	5.36	0.013
	4	−25	31	R middle cingulate gyrus	5.13	0.029
342	−15	−19	18	L thalamus	5.39	0.011
	−18	−25	13	L thalamus	5.34	0.014
113	64	−47	−21	R inferior temporal gyrus	5.50	0.008
COVID-OD						
3526	23	7	−1	R putamen	7.56	<0.001
2801	−26	4	4	L putamen	6.67	<0.001
	−24	8	−5	L putamen	6.22	< 0.001
1683	−16	−27	13	L thalamus	5.83	<0.001
	−12	−5	17	L caudate	5.82	0.001
1523	6	−21	50	R precentral gyrus (medial segment)	6.71	<0.001
	2	−31	54	R precentral gyrus (medial segment)	6.14	<0.001
	2	−13	71	R supplementary motor cortex	5.26	0.012
947	20	−49	−13	Cerebellar vermal lobules I–V	5.81	0.001
	22	−42	−20	R cerebellum exterior	4.97	0.035
889	21	−58	3	R lingual gyrus	5.91	<0.001
	17	−60	11	R cuneus	5.24	0.013
690	31	−12	−19	R hippocampus	5.56	0.004
554	−5	−19	72	L precentral gyrus (medial segment)	6.01	0.001
530	10	1	15	R caudate	5.91	0.001
465	14	−25	13	R thalamus	5.59	0.003
375	−3	−29	52	L precentral gyrus (medial segment)	5.94	0.001
182	−30	−22	63	L precentral gyrus	5.71	0.002

GM regions were defined using the Neuromorphometrics atlas (Neuromorphometrics, Inc. http://Neuromorphometrics.com/). Reading example: the first line denotes the presence of a 3D cluster made of 16627 contiguous voxels of significant atrophy in COVID-CD group as compared to controls. The most significant voxel of the cluster has stereotactic coordinates of (23, −48, −13) and is located in the right fusiform gyrus. Within the same cluster there are two other peaks of significance distant more than 8 mm from the former and located at (4, −21, 50) and (−2, −28, 46), falling within the medial segment of the right precentral gyrus and in the left posterior cingulate gyrus, respectively.
Abbreviations: CD, cognitive disorders; FWE, family-wise error; L, left, OD, olfactory disorders; R, right.

 © 2024 The Author(s). *Annals of Clinical and Translational Neurology* published by Wiley Periodicals LLC on behalf of American Neurological Association.

cortical thickness ($p < 0.05$, FWE-corrected, cluster-extent threshold = 20 vertices), mainly in the medial part of both brain hemispheres. The largest clusters with significantly thinner cortex are centered in the bilateral paracentral lobule and in the right lingual gyrus.

Table 4 details the group differences in terms of T-statistics, while Figure 3 provides a graphical representation of the results on the FreeSurfer FsAverage surface.

No statistically significant increase in cortical thickness was found in either the COVD-CD or the COVID-OD group when compared to controls.

Discussion

In this study, we investigated GM structural alterations in a dual population of COVID-19 patients exhibiting the most highly prevalent COVID-19-related neurological symptoms – cognitive disorders as primary neurological manifestation (COVID-CD) or olfactory impairments as sole neurological complication (COVID-OD) – as compared to a control population, using a multimorphometric approach.

The analysis, accounting for age and sex differences, showed statistically significant GM loss and reduced cortical thickness in both COVID-CD and COVID-OD patient groups when compared to normal controls. Specifically, COVID-CD patients exhibited a more pronounced and more widespread tissue depletion than COVID-OD patients, suggesting that in patients with cognitive disorders SARS-CoV-2 triggered a stronger inflammatory response than in those experiencing loss of smell as sole neurological symptom.

At a regional level, COVID-CD patients exhibited statistically significant volume reduction in 73 GM regions, mainly in the hippocampus, the putamen, the cingulate, the precuneus, the precentral and postcentral gyri, the amygdala, the lingual gyrus, and the caudate nucleus. These regions, also showing lower GM density and/or cortical thinning, are known to be associated with memory impairment, which was the most recurring symptom in COVID-CD patients.

Different types of memory can be impaired, alternatively or in combination, pointing to the involvement of multiple brain systems. The putamen and caudate nucleus, collectively referred to as the striatum, sit at a key location in the motor loop, and have been shown to be critical for the procedural memory.[74,75] Within the medial temporal lobe, the hippocampus is mostly involved in episodic memory.[74–77] The precuneus, as well as some surrounding areas including the posterior cingulate, is believed to play a crucial role in episodic memory retrieval.[78,79] Recognition memory is thought to be handled by the diencephalon, especially by the anterior and dorsomedial nuclei in the thalamus and the mammillary bodies in the hypothalamus.[74,80] Lastly, atrophy of the amygdala has been shown to associate with the severity of cognitive impairment at early stages of dementia[81] and, being one of the most widely connected regions of the brain, is considered to play a crucial role in prioritization of declarative memories[82] as well as in memory for emotional experiences.[74]

Besides memory impairment, many COVID-CD patients also reported attention deficits. The thalamus, apart from being associated with high-level cognition – working memory, rule-based learning, and decision making – is also thought to be involved in directing attention.[83] Furthermore, individuals with damage to the pulvinar region of the thalamus were found to exhibit atypically delayed responses to stimuli, which may indicate a diminished capacity to concentrate attention on objects.[74] In line with these findings, we found the thalamus to be atrophic in the COVID-CD patient group as compared to controls.

COVID-OD patients exhibited a statistically significant volume reduction in 41 regions, all of which were also found atrophic in the COVID-CD group. This overlap can be explained by the fact that, same as for other senses, olfactory abilities rely on both sensory and cognitive processes,[84] with many GM regions being involved in both. Odorants bind to receptors of olfactory sensory neurons, which project to the olfactory bulbs that in turn directly connect to the primary olfactory cortex. This process encompasses various regions of the medial temporal and basal frontal lobe, such as the piriform cortex (which comprises the uncus and the anterior parahippocampal gyrus) and the amygdala, both intimately associated to memory functions.[85] Previous evidence also suggested that the hippocampus may play a crucial role in integrating information derived from multiple sensory and cognitive sources to generate associative and explicit memory.[86] The interconnection between olfactory identification and spatial memory is thought to be attributed to shared brain regions, including the orbitofrontal cortex and – again – the hippocampus.[87] Moreover, according to Cerf-Ducastel and Murphy,[88] the right hippocampus, parahippocampal, lingual, fusiform and middle frontal gyrus might play a specific role in olfactory recognition memory.

Such close anatomical connection between olfactory and memory structures is believed to make odor exposure a powerful trigger for memory retrieval and emotion.[89] Our findings, showing significant cortical thinning in the parahippocampal gyrus and notable atrophy of the amygdala and hippocampus in both COVID-19 patient groups, is in line with this widely acknowledged hypothesis.

Finally, it has long been known that olfactory loss is a common feature accompanying cognitive impairment or

© 2024 The Author(s). *Annals of Clinical and Translational Neurology* published by Wiley Periodicals LLC on behalf of American Neurological Association.

Table 4. Clusters of brain cortex vertices with significant thickness reduction in the patient groups as compared to controls ($p < 0.05$, FWE-corrected; extent threshold = 20 vertices).

	Peak MNI coordinates (mm)					
Cluster size	*x*	*y*	*z*	Region	*T*	*p*
COVID-CD						
2580	10	−22	48	R paracentral lobule	7.57	<0.001
	3	−33	30	R isthmus-cingulate cortex	7.06	<0.001
	6	−56	30	R precuneus cortex	6.65	<0.001
2557	−7	−22	56	L paracentral lobule	7.30	<0.001
	−4	−24	42	L posterior-cingulate cortex	6.83	<0.001
	−33	−20	46	L precentral gyrus	6.73	< 0.001
587	26	−59	−7	R lingual gyrus	7.42	<0.001
	28	−43	−9	R lingual gyrus	5.60	0.001
	7	−61	4	R lingual gyrus	4.95	0.010
327	−27	−13	60	L precentral gyrus	5.52	0.001
	−27	5	52	L caudal middle frontal gyrus	5.29	0.003
	−28	−3	46	L caudal middle frontal gyrus	5.22	0.004
322	35	−65	48	R superior parietal cortex	5.85	<0.001
	34	−49	38	R inferior parietal cortex	5.35	0.002
208	46	−32	41	R supramarginal gyrus	6.53	<0.001
201	−14	−40	−1	L isthmus-cingulate cortex	5.59	0.001
	−15	−50	−4	L lingual gyrus	5.47	0.002
199	36	11	35	R caudal middle frontal gyrus	5.60	0.001
	34	12	26	R pars opercularis	5.52	0.001
169	35	−23	45	R precentral gyrus	5.21	0.004
	36	−27	51	R postcentral gyrus	4.96	0.010
153	29	−23	61	R precentral gyrus	5.61	0.001
76	−48	−43	26	L supramarginal gyrus	5.61	0.001
61	48	−39	−23	R inferior temporal gyrus	6.09	<0.001
58	30	−25	−27	R parahippocampal gyrus	5.11	0.006
51	−17	−75	29	L precuneus cortex	4.92	0.011
50	51	−36	20	R superior temporal gyrus	5.46	0.002
50	52	−20	55	R postcentral gyrus	4.79	0.017
42	−30	−64	−16	L fusiform gyrus	5.43	0.002
41	−40	−1	35	L precentral gyrus	4.83	0.015
34	23	−3	63	R superior frontal gyrus	4.59	0.034
	22	−10	58	R precentral gyrus	4.55	0.038
33	59	−50	−20	R inferior temporal gyrus	5.22	0.004
28	−55	−2	6	L precentral gyrus	4.86	0.014
28	57	−2	39	R precentral gyrus	4.78	0.018
26	30	−2	47	R caudal middle frontal gyrus	4.68	0.025
24	−22	−61	7	L precuneus cortex	4.84	0.015
22	42	−11	−31	R inferior temporal gyrus	5.03	0.008
COVID-OD						
3073	7	−20	49	R paracentral lobule	8.81	<0.001
	16	−81	34	R superior parietal cortex	6.77	<0.001
	7	−31	29	R isthmus-cingulate cortex	6.32	<0.001
1415	−4	−14	52	L paracentral lobule	6.67	<0.001
	−3	−20	41	L posterior-cingulate cortex	6.54	<0.001
	−5	−58	22	L precuneus cortex	6.43	<0.001
328	26	−59	−7	R lingual gyrus	6.48	<0.001
	24	−41	−11	R parahippocampal gyrus	5.01	0.005
229	−24	−24	61	L precentral gyrus	5.50	0.001
	−34	−21	48	L precentral gyrus	5.18	0.003
	−15	−28	65	L precentral gyrus	4.97	0.006
163	−48	−10	26	L postcentral gyrus	5.11	0.004

(*Continued*)

 © 2024 The Author(s). *Annals of Clinical and Translational Neurology* published by Wiley Periodicals LLC on behalf of American Neurological Association.

Table 4 Continued.

Cluster size	Peak MNI coordinates (mm)			Region	*T*	*p*
	x	*y*	*z*			
	−40	−15	35	L precentral gyrus	5.01	0.005
91	43	−30	39	R supramarginal gyrus	5.48	0.001
90	−11	−48	1	L isthmus-cingulate cortex	5.07	0.004
32	−12	−70	−8	L lingual gyrus	4.91	0.008
27	32	−21	−30	R parahippocampal gyrus	4.84	0.010
27	33	−50	38	R inferior parietal cortex	4.78	0.012
24	42	−11	−34	R inferior temporal gyrus	4.67	0.018

Regions of the cerebral cortex were defined using the Desikan-Killiany atlas.[68] Reading example: the first line denotes the presence of a 3D cluster made of 2580 contiguous vertices of significant cortex thinning in COVID-CD group as compared to controls. The most significant vertex of the cluster has stereotactic coordinates of (10, −22, 48) and is located in the right paracentral lobule. Within the same cluster there are two other peaks of significance distant more than 8 mm from the former and located at (3, −33, 30) and (6, −56, 30), falling in the right isthmus-cingulate cortex and in the right precuneus cortex, respectively.

Abbreviations: CD, cognitive disorders; FWE, family-wise error; L, left, OD, olfactory disorders; R, right.

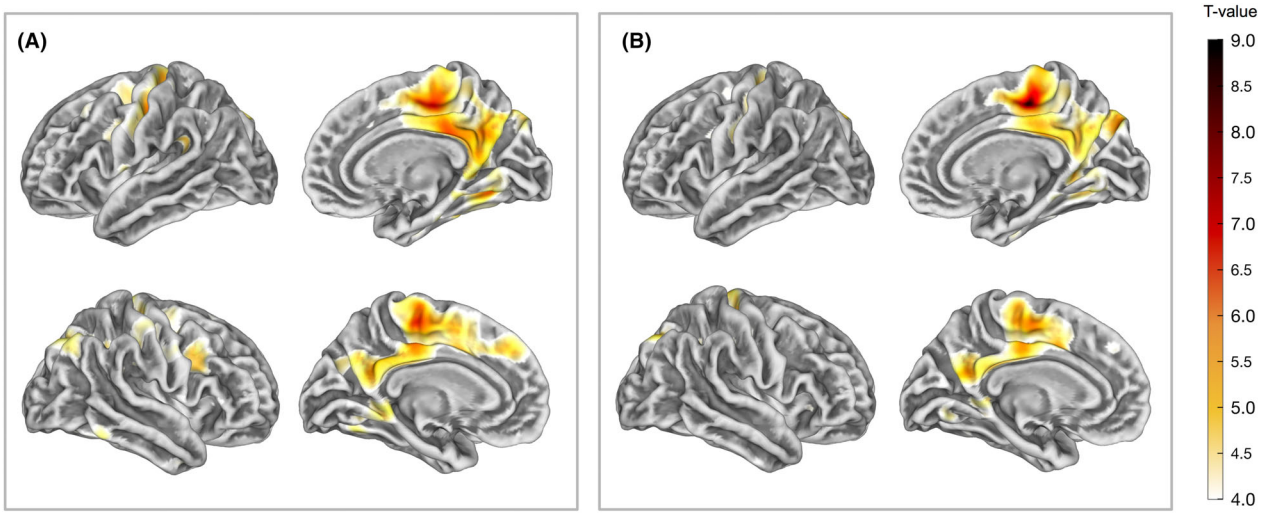

Figure 3. Statistically significant cortical thinning in the 61 COVID-19 patients with cognitive disorders (COVID-CD) (A) and in the 84 COVID-19 patients with olfactory dysfunction (COVID-OD) (B), as compared to controls. Significant vertex-wise difference is color-coded based on statistical significance (FWE-corrected *p*-value <0.05). Cluster extent threshold was set at 20 vertices. Age was included as covariate in the GLM. The color-coded findings are superimposed on the FreeSurfer FsAverage surface, in the lateral and medial views.

dementia (especially Alzheimer's and Parkinson's diseases),[90] with several studies showing that olfactory deficits often coincide with or even precede impairments in nonolfactory cognitive tests.[84] In particular, Kjelvik et al.[91] reported significantly smaller hippocampal volume in patients with amnestic mild cognitive impairment or early Alzheimer's disease with reduced odor identification ability, as well as a significant association between odor identification scores and hippocampal volume. This may further explain the fact that numerous GM regions showed reduced volume in both the COVID-CD and COVID-OD groups.

Our findings are also in line with previous studies showing reduced GM volume and/or cortical thinning in COVID-19 patients with subjective cognitive complaints,[59] depression and post-traumatic distress,[57] fatigue,[92,93] persistent headache,[62] and olfactory dysfunction,[58,94] as well as in COVID-19 patients with heterogeneous neurological symptoms.[55,61,95,96] In particular, GM atrophy in the limbic system has been consistently observed.

The main added value of this study is that, to the best of our knowledge, it is the first one comprehensively investigating GM structural alterations in two distinct and well-defined subgroups of COVID-19 patients exhibiting

© 2024 The Author(s). *Annals of Clinical and Translational Neurology* published by Wiley Periodicals LLC on behalf of American Neurological Association.

very different – although both highly prevalent –neurological disorders. A further strength is the adoption of a multi-morphometric approach, encompassing RBM, VBM, and SBM, providing complementary information, and thus allowing to obtain comprehensive and solid results on brain structural alterations. ROI analyses (RBM) are denoted by low sensitivity to effects occurring at a fine spatial scale, such as within specific subregions. On the other hand, VBM allows to objectively investigate tissue density with an exceptional level of regional specificity at the voxel level,[97] but it is more dependent on the quality of MR images, which can lower its accuracy. According to Dusi et al.[98] the ROI approach is a confirmatory analysis for the validation of VBM findings.

The main limitation of the present study is the small number of controls, which was mainly due to technical reasons. For MRI protocol consistency, it was not possible to include controls with MRI scans acquired on scanners different from the one used for COVID-19 patients or with very different acquisition parameters, although minor differences were unavoidable due to the retrospective nature of the study. However, as controls are expected to have lower variability than patients, the choice of including fewer controls than COVID-19 patients was justifiable. Second, since patients were retrospectively enrolled, the MRI time was heterogeneous, although not statistically significantly different between COVID-19 patient groups. Last, this study was also limited by the lack of neuropsychological tests allowing to evaluate the severity of cognitive impairment in the COVID-CD group, as well as the lack of smell tests to assess the degree of olfactory dysfunction in the COVID-OD group. This prevented the stratification of the cases and the investigation of possible correlations between the severity of cognitive or olfactory disorder and varying degrees of GM atrophy.

Future longitudinal studies are needed to investigate GM structure alterations' trend overtime and clarify their transient or permanent nature, as well as to investigate possible correlations between brain structural alterations and the severity of neurological symptoms in COVID-19.

Conclusion

In conclusion, our multi-morphometric MRI analysis revealed that COVID-19 induces GM atrophy in both patients with olfactory and cognitive disorders, with the latter group exhibiting more extensive and severe structural alterations. The affected regions, which include the hippocampus, putamen, cingulate gyrus, and amygdala among others, are critical for cognitive functions and olfactory processing. These findings suggest that the neurological impact of COVID-19 may be driven by underlying neurodegeneration and neuroinflammation, with cognitive symptoms being associated with more pronounced brain damage.

Acknowledgments

We extend our sincere appreciation to Cristina Casalini, the radiology technician responsible for acquiring most MRIs during the initial phase of the pandemic, as well as the dedicated nurses and technicians from the Neuroradiology Unit, whose commitment and support were crucial in caring for these patients, particularly during the pandemic's early stages.

Funding Information

The study was supported in part by a grant from Brembo SpA (Curno, Bergamo, Italy), under the initiative "Progetto TrexUno."

Conflict of Interest

The authors report no conflicts of interest relevant to the research presented in this study.

Author Contributions

SC, AC, and SG contributed to the conception of the study. SC, AC, AA, AN, GP, AR, LGL, FLL, MS, and SG contributed to the design of the study. SC, AC, and AA contributed to the analysis of the data. AN and GP contributed to the acquisition of data. SC, AC, AA, AN, GP, AR, LGL, FLL, MS, and SG contributed to the interpretation of the data. SC and AC drafted the article. AA, AN, GP, AR, LGL, FLL, MS, and SG provided critical revisions to the manuscript, ultimately approving the final version of the document.

Data Availability Statement

The data that support the findings of this study are available from the corresponding author, upon reasonable request.

References

1. Pezzini A, Padovani A. Lifting the mask on neurological manifestations of COVID-19. Nat Rev Neurol. 2020;16 (11):636-644.
2. Ellul MA, Benjamin L, Singh B, et al. Neurological associations of COVID-19. Lancet Neurol. 2020;19 (9):767-783.
3. Pergolizzi JV, Raffa RB, Varrassi G, et al. Potential neurological manifestations of COVID-19: a narrative review. Postgrad Med. 2022;134(4):395-405.

 © 2024 The Author(s). *Annals of Clinical and Translational Neurology* published by Wiley Periodicals LLC on behalf of American Neurological Association.

4. Johansson A, Mohamed MS, Moulin TC, Schiöth HB. Neurological manifestations of COVID-19: a comprehensive literature review and discussion of mechanisms. J Neuroimmunol. 2021;358:577658.
5. Favas TT, Dev P, Chaurasia RN, et al. Neurological manifestations of COVID-19: a systematic review and meta-analysis of proportions. Neurol Sci. 2020;41 (12):3437-3470.
6. Sarubbo F, El Haji K, Vidal-Balle A, Bargay LJ. Neurological consequences of COVID-19 and brain related pathogenic mechanisms: a new challenge for neuroscience. Brain Behav Immun Health. 2022;19:100399.
7. Kumar PR, Shilpa B, Jha RK. Brain disorders: impact of mild SARS-CoV-2 may shrink several parts of the brain. Neurosci Biobehav Rev. 2023;149:105150.
8. Sonneville R, Dangayach NS, Newcombe V. Neurological complications of critically ill COVID-19 patients. Curr Opin Crit Care. 2023;29(2):61-67.
9. Ludwig B, Deckert M, Krajnc N, et al. Reported neurological symptoms after severe acute respiratory syndrome coronavirus type 2 infection: a systematic diagnostic approach. Eur J Neurol. 2023;30:2713-2725.
10. Hosp JA, Dressing A, Blazhenets G, et al. Cognitive impairment and altered cerebral glucose metabolism in the subacute stage of COVID-19. Brain. 2021;144:1263-1276.
11. Graham EL, Clark JR, Orban ZS, et al. Persistent neurologic symptoms and cognitive dysfunction in non-hospitalized Covid-19 "long haulers". Ann Clin Transl Neurol. 2021;8(5):1073-1085.
12. Crook H, Ramirez A, Hosseini A, et al. European working group on SARS-CoV-2: current understanding, unknowns, and recommendations on the neurological complications of COVID-19. Brain Connect. 2023;13(4):178-210.
13. Vanderlind WM, Rabinovitz BB, Miao IY, et al. A systematic review of neuropsychological and psychiatric sequalae of COVID-19: implications for treatment. Curr Opin Psychiatry. 2021;34(4):420-433.
14. Soltani S, Tabibzadeh A, Zakeri A, et al. COVID-19 associated central nervous system manifestations, mental and neurological symptoms: a systematic review and meta-analysis. Rev Neurosci. 2021;32(3):351-361.
15. Choi Y, Lee MK. Neuroimaging findings of brain MRI and CT in patients with COVID-19: a systematic review and meta-analysis. Eur J Radiol. 2020;133:109393.
16. Moonis G, Filippi CG, Kirsch CFE, et al. The Spectrum of neuroimaging findings on CT and MRI in adults with COVID-19. Am J Roentgenol. 2021;217(4):959-974.
17. Ladopoulos T, Zand R, Shahjouei S, et al. COVID-19: neuroimaging features of a pandemic. J Neuroimaging. 2021;31(2):228-243.
18. Alhazmi FH, Alsharif WM, Alshoabi SA, et al. Identifying cerebral microstructural changes in patients with COVID-19 using MRI: a systematic review. Brain Circ. 2023;9 (1):6-15.
19. Najt P, Richards HL, Fortune DG. Brain imaging in patients with COVID-19: a systematic review. Brain Behav Immun Health. 2021;16:100290.
20. Ghaderi S, Olfati M, Ghaderi M, et al. Neurological manifestation in COVID-19 disease with neuroimaging studies. Am J Neurodegener Dis. 2023;12(2):42-84.
21. Faro SH, Manmatharayan A, Leiby B, et al. Neuroimaging findings in 4342 hospitalized COVID-19 subjects: a multicenter report from the United States and Europe. J Neuroimaging. 2023;33:752-763.
22. Parsons N, Outsikas A, Parish A, et al. Modelling the anatomic distribution of neurologic events in patients with COVID-19: a systematic review of MRI findings. AJNR Am J Neuroradiol. 2021;42(7):1190-1195.
23. Katal S, Balakrishnan S, Gholamrezanezhad A. Neuroimaging and neurologic findings in COVID-19 and other coronavirus infections: a systematic review in 116 patients. J Neuroradiol. 2021;48(1):43-50.
24. Chen B, Chen C, Zheng J, Li R, Xu J. Insights into neuroimaging findings of patients with coronavirus disease 2019 presenting with neurological manifestations. Front Neurol. 2020;11:593520. doi:10.3389/fneur.2020.593520
25. Caroli A, Capelli S, Napolitano A, et al. Brain diffusion alterations in patients with COVID-19 pathology and neurological manifestations. NeuroImage: Clinical. 2023;37:103338.
26. Capelli S, Caroli A, Barletta A, et al. MRI evidence of olfactory system alterations in patients with COVID-19 and neurological symptoms. J Neurol. 2023;270:1195-1206. doi:10.1007/s00415-023-11561-0
27. Napolitano A, Arrigoni A, Caroli A, et al. Cerebral microbleeds assessment and quantification in COVID-19 patients with neurological manifestations. Front Neurol. 2022;13:884449. doi:10.3389/fneur.2022.884449
28. Muccioli L, Sighinolfi G, Mitolo M, et al. Cognitive and functional connectivity impairment in post-COVID-19 olfactory dysfunction. NeuroImage: Clinical. 2023;38:103410.
29. Arrigoni A, Previtali M, Bosticardo S, et al. Brain microstructure and connectivity in COVID-19 patients with olfactory or cognitive impairment. NeuroImage: Clinical. 2024;43:103631.
30. Mutiawati E, Fahriani M, Mamada SS, et al. Anosmia and dysgeusia in SARS-CoV-2 infection: incidence and effects on COVID-19 severity and mortality, and the possible pathobiology mechanisms - a systematic review and meta-analysis. F1000Res. 2021;10:40.
31. Butowt R, von Bartheld CS. Anosmia in COVID-19: underlying mechanisms and assessment of an olfactory route to brain infection. Neuroscientist. 2021;27 (6):582-603.
32. Karamali K, Elliott M, Hopkins C. COVID-19 related olfactory dysfunction. Curr Opin Otolaryngol Head Neck Surg. 2022;30(1):19-25. https://journals.lww.com/co-

© 2024 The Author(s). *Annals of Clinical and Translational Neurology* published by Wiley Periodicals LLC on behalf of American Neurological Association.

otolaryngology/Fulltext/2022/02000/COVID_19_related_olfactory_dysfunction.5.aspx
33. Dubé M, le Coupanec A, Wong AHM, Rini JM, Desforges M, Talbot PJ. Axonal transport enables neuron-to-neuron propagation of human coronavirus OC43. J Virol. 2018;92(17):e00404-18.
34. Guo P, Benito Ballesteros A, Yeung SP, et al. COVCOG 2: cognitive and memory deficits in long COVID: a second publication from the COVID and cognition study. Front Aging Neurosci. 2022;14:804937. doi:10.3389/fnagi.2022.804937
35. Gonzalez-Fernandez E, Huang J. Cognitive aspects of COVID-19. Curr Neurol Neurosci Rep. 2023;23:531-538. doi:10.1007/s11910-023-01286-y
36. Hampshire A, Azor A, Atchison C, et al. Cognition and memory after Covid-19 in a large community sample. N Engl J Med. 2024;390(9):806-818.
37. Widmann CN, Wieberneit M, Bieler L, et al. Longitudinal neurocognitive and Pulmonological profile of long COVID-19: protocol for the COVIMMUNE-Clin study. JMIR Res Protoc. 2021;10(11):e30259.
38. Matsuda H. Morphometry in normal aging. In: Spalletta G, Piras F, Gili T, eds. Brain Morphometry. Springer; 2018:165-181. doi:10.1007/978-1-4939-7647-8_11
39. Ramanoël S, Hoyau E, Kauffmann L, et al. Gray matter volume and cognitive performance during Normal aging. A voxel-based morphometry study. Front Aging Neurosci. 2018;10:235.
40. Lipp I, Muhlert N, Tomassini V. Brain morphometry in multiple sclerosis. In: Spalletta G, Piras F, Gili T, eds. Brain Morphometry. Springer; 2018:279-300. doi:10.1007/978-1-4939-7647-8_17
41. Di Paola M, Bourisly AK. Structural MRI in neurodegenerative non-Alzheimer's dementia. In: Spalletta G, Piras F, Gili T, eds. Brain Morphometry. Springer; 2018:241-265. doi:10.1007/978-1-4939-7647-8_15
42. De Marco M, Venneri A. Brain morphometry: Alzheimer's disease. In: Spalletta G, Piras F, Gili T, eds. Brain Morphometry. Springer; 2018:217-240. doi:10.1007/978-1-4939-7647-8_14
43. Péran P, Nemmi F, Barbagallo G. Brain morphometry: Parkinson's disease. In: Spalletta G, Piras F, Gili T, eds. Brain Morphometry. Springer; 2018:267-277. doi:10.1007/978-1-4939-7647-8_16
44. Dahnke R, Gaser C. Surface and shape analysis. In: Spalletta G, Piras F, Gili T, eds. Brain Morphometry. Springer; 2018:51-73. doi:10.1007/978-1-4939-7647-8_4
45. Matsuda H. Voxel-based morphometry of brain MRI in Normal aging and Alzheimer's disease. Aging Dis. 2012;4(1):29-37.
46. Matsuda H. MRI morphometry in Alzheimer's disease. Ageing Res Rev. 2016;30:17-24.
47. Hirata Y, Matsuda H, Nemoto K, et al. Voxel-based morphometry to discriminate early Alzheimer's disease from controls. Neurosci Lett. 2005;382(3):269-274.
48. Ashburner J. Computational anatomy with the SPM software. Magn Reson Imaging. 2009;27(8):1163-1174.
49. Gaser C, Dahnke R, Thompson PM, et al. CAT – a computational anatomy toolbox for the analysis of structural MRI data. 2022;2022.06.11.495736. doi:10.1101/2022.06.11.495736v1
50. Whitwell JL. Voxel-based morphometry: an automated technique for assessing structural changes in the brain. J Neurosci. 2009;29(31):9661-9664.
51. Ashburner J, Friston KJ. Voxel-based morphometry—the methods. NeuroImage. 2000;11(6 Pt 1):805-821.
52. Kurth F, Luders E, Gaser C. Voxel-based morphometry. In: Toga AW, ed. Brain Mapping. Academic Press; 2015:345-349. https://www.sciencedirect.com/science/article/pii/B9780123970251003043
53. Mechelli A, Price JC, Friston JK, Ashburner J. Voxel-based morphometry of the human brain: methods and applications. Current Medical Imaging. 2005;1(2):105-113.
54. Goto M, Abe O, Hagiwara A, et al. Advantages of using both voxel- and surface-based morphometry in cortical morphology analysis: a review of various applications. Magn Reson Med Sci. 2022;21(1):41-57.
55. Douaud G, Lee S, Alfaro-Almagro F, et al. SARS-CoV-2 is associated with changes in brain structure in UK biobank. Nature. 2022;604(7907):697-707.
56. Du Y, Zhao W, Huang S, et al. Two-year follow-up of brain structural changes in patients who recovered from COVID-19: a prospective study. Psychiatry Res. 2023;319:114969.
57. Benedetti F, Palladini M, Paolini M, et al. Brain correlates of depression, post-traumatic distress, and inflammatory biomarkers in COVID-19 survivors: a multimodal magnetic resonance imaging study. Brain Behav Immun Health. 2021;18:100387.
58. Campabadal A, Oltra J, Junqué C, et al. Structural brain changes in post-acute COVID-19 patients with persistent olfactory dysfunction. Ann Clin Transl Neurol. 2023;10(2):195-203.
59. Díez-Cirarda M, Yus M, Gómez-Ruiz N, et al. Multimodal neuroimaging in post-COVID syndrome and correlation with cognition. Brain. 2022;146:2142-2152.
60. Rothstein TL. Cortical grey matter volume depletion links to neurological sequelae in post COVID-19 "long haulers". BMC Neurol. 2023;23(1):22.
61. Sanabria-Diaz G, Etter MM, Melie-Garcia L, et al. Brain cortical alterations in COVID-19 patients with neurological symptoms. Front Neurosci. 2022;16:992165. doi:10.3389/fnins.2022.992165
62. Planchuelo-Gómez Á, García-Azorín D, Guerrero ÁL, Rodríguez M, Aja-Fernández S, de Luis-García R.

 © 2024 The Author(s). *Annals of Clinical and Translational Neurology* published by Wiley Periodicals LLC on behalf of American Neurological Association.

Structural brain changes in patients with persistent headache after COVID-19 resolution. J Neurol. 2023;270 (1):13-31.
63. Whitcroft KL, Hummel T. Olfactory dysfunction in COVID-19: diagnosis and management. JAMA. 2020;323 (24):2512-2514.
64. Rajapakse JC, Giedd JN, Rapoport JL. Statistical approach to segmentation of single-channel cerebral MR images. IEEE Trans Med Imaging. 1997;16(2):176-186.
65. Tohka J, Zijdenbos A, Evans A. Fast and robust parameter estimation for statistical partial volume models in brain MRI. NeuroImage. 2004;23(1):84-97.
66. Ashburner J, Friston KJ. Diffeomorphic registration using geodesic shooting and gauss–Newton optimisation. NeuroImage. 2011;55(3):954-967.
67. Dahnke R, Yotter RA, Gaser C. Cortical thickness and central surface estimation. NeuroImage. 2013;65:336-348.
68. Desikan RS, Ségonne F, Fischl B, et al. An automated labeling system for subdividing the human cerebral cortex on MRI scans into gyral based regions of interest. NeuroImage. 2006;31(3):968-980.
69. Pernet CR. The general linear model: theory and practicalities in brain morphometric analyses. Brain Morphometry: Methods and Clinical Applications. Springer; 2018:75-85. https://www.research.ed.ac.uk/en/publications/the-general-linear-model-theory-and-practicalities-in-brain-morph
70. Whitwell JL, Crum WR, Watt HC, Fox NC. Normalization of cerebral volumes by use of intracranial volume: implications for longitudinal quantitative MR imaging. AJNR Am J Neuroradiol. 2001;22(8):1483-1489.
71. Henley SMD, Ridgway GR, Scahill RI, et al. Pitfalls in the use of voxel-based morphometry as a biomarker: examples from huntington disease. AJNR Am J Neuroradiol. 2010;31(4):711-719.
72. Barnes J, Ridgway GR, Bartlett J, et al. Head size, age and gender adjustment in MRI studies: a necessary nuisance? NeuroImage. 2010;53(4):1244-1255.
73. Poldrack RA, Mumford JA. Independence in ROI analysis: where is the voodoo? Soc Cogn Affect Neurosci. 2009;4 (2):208-213.
74. Bear MF, Connors BW, Paradiso MA. Neuroscience: Exploring the Brain. 3rd ed. Lippincott Williams & Wilkins Publishers; 2007.
75. Ferbinteanu J. Contributions of hippocampus and striatum to memory-guided behavior depend on past experience. J Neurosci. 2016;36(24):6459-6470.
76. Bird CM, Burgess N. The hippocampus and memory: insights from spatial processing. Nat Rev Neurosci. 2008;9 (3):182-194.
77. Dekeyzer S, De Kock I, Nikoubashman O, et al. "Unforgettable" – a pictorial essay on anatomy and pathology of the hippocampus. Insights Imaging. 2017;8 (2):199-212.
78. Cavanna AE, Trimble MR. The precuneus: a review of its functional anatomy and behavioural correlates. Brain. 2006;129(Pt 3):564-583.
79. Trimble MR, Cavanna AE. Chapter 3.7 the role of the precuneus in episodic memory. In: Dere E, Easton A, Nadel L, Huston JP, eds. Handbook of Behavioral Neuroscience. Elsevier; 2008:363-377. https://www.sciencedirect.com/science/article/pii/S1569733908002208
80. Aggleton JP, Dumont JR, Warburton EC. Unraveling the contributions of the diencephalon to recognition memory: a review. Learn Mem. 2011;18(6):384-400.
81. Poulin SP, Dautoff R, Morris JC, Barrett LF, Dickerson BC. Amygdala atrophy is prominent in early Alzheimer's disease and relates to symptom severity. Psychiatry Res Neuroimaging. 2011;194(1):7-13.
82. Manns JR, Bass DI. The amygdala and prioritization of declarative memories. Curr Dir Psychol Sci. 2016;25 (4):261-265.
83. de Bourbon-Teles J, Bentley P, Koshino S, et al. Thalamic control of human attention driven by memory and learning. Curr Biol. 2014;24(9):993-999.
84. Olofsson JK, Ekström I, Larsson M, Nordin S. Olfaction and aging: a review of the current state of research and future directions. Iperception. 2021;12 (3):20416695211020331.
85. Carlson H, Leitão J, Delplanque S, Cayeux I, Sander D, Vuilleumier P. Sustained effects of pleasant and unpleasant smells on resting state brain activity. Cortex. 2020;132:386-403.
86. Strauch C, Manahan-Vaughan D. Orchestration of hippocampal information encoding by the piriform cortex. Cereb Cortex. 2020;30(1):135-147.
87. Dahmani L, Patel RM, Yang Y, Chakravarty MM, Fellows LK, Bohbot VD. An intrinsic association between olfactory identification and spatial memory in humans. Nat Commun. 2018;9:4162.
88. Cerf-Ducastel B, Murphy C. Neural substrates of cross-modal olfactory recognition memory: an fMRI study. NeuroImage. 2006;31(1):386-396.
89. Saive A-L, Royet J-P, Plailly J. A review on the neural bases of episodic odor memory: from laboratory-based to autobiographical approaches. Front Behav Neurosci. 2014;8:240.
90. Hawkes C. Olfaction in neurodegenerative disorder. Adv Otorhinolaryngol. 2006;63:133-151.
91. Kjelvik G, Saltvedt I, White LR, et al. The brain structural and cognitive basis of odor identification deficits in mild cognitive impairment and Alzheimer's disease. BMC Neurol. 2014;14:168.
92. Bispo DD d C, Brandão PR d P, Pereira DA, et al. Brain microstructural changes and fatigue after COVID-19. Front Neurol. 2022;13:1029302. doi:10.3389/fneur.2022.1029302
93. Hafiz R, Gandhi TK, Mishra S, et al. Higher limbic and basal ganglia volumes in surviving COVID-negative

© 2024 The Author(s). *Annals of Clinical and Translational Neurology* published by Wiley Periodicals LLC on behalf of American Neurological Association.

patients and the relations to fatigue. Neuroimage: Reports. 2022;2(2):100095.
94. Postma EM, Smeets P a M, Boek WM, Boesveldt S. Investigating morphological changes in the brain in relation to etiology and duration of olfactory dysfunction with voxel-based morphometry. Sci Rep. 2021;11(1):12704.
95. Bendella Z, Widmann CN, Layer JP, et al. Brain volume changes after COVID-19 compared to healthy controls by artificial intelligence-based MRI Volumetry. Diagnostics. 2023;13(10):1716.
96. Nouraeinejad A. The functional and structural changes in the hippocampus of COVID-19 patients. Acta Neurol Belg. 2023;123(4):1247-1256.
97. Kurth F, Gaser C, Luders E. A 12-step user guide for analyzing voxel-wise gray matter asymmetries in statistical parametric mapping (SPM). Nat Protoc. 2015;10(2):293-304.
98. Dusi N, Delvecchio G, Rovera C, et al. Voxel-based morphometry imaging studies in major depression. In: Spalletta G, Piras F, Gili T, eds. Brain Morphometry. Springer; 2018:385-402. doi:10.1007/978-1-4939-7647-8_21

Supporting Information

Additional supporting information may be found online in the Supporting Information section at the end of the article.

Appendix S1.

 © 2024 The Author(s). *Annals of Clinical and Translational Neurology* published by Wiley Periodicals LLC on behalf of American Neurological Association.